

See discussions, stats, and author profiles for this publication at: <https://www.researchgate.net/publication/230594030>

Langmuir Monolayers of an Inclusion Complex Formed by a New Calixarene Derivative and Fullerene

ARTICLE *in* LANGMUIR · AUGUST 2012

Impact Factor: 4.46 · DOI: 10.1021/la302440g · Source: PubMed

CITATIONS

6

READS

57

5 AUTHORS, INCLUDING:



[Juan Giner-Casares](#)

CIC biomaGUNE

46 PUBLICATIONS 282 CITATIONS

SEE PROFILE



[Jean-Bernard Regnouf-de-Vains](#)

University of Lorraine

84 PUBLICATIONS 1,016 CITATIONS

SEE PROFILE



[Luis Camacho](#)

University of Cordoba (Spain)

150 PUBLICATIONS 1,564 CITATIONS

SEE PROFILE

Langmuir Monolayers of an Inclusion Complex Formed by a New Calixarene Derivative and Fullerene

Antonio M. González-Delgado,[†] Juan J. Giner-Casares,^{†,b} Gerald Brezesinski,^b Jean-Bernard Regnoui-de-Vains,^c and Luis Camacho^{†,*}

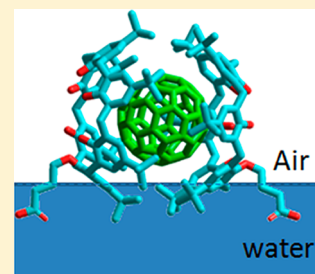
[†]Department of Physical Chemistry and Applied Thermodynamics, University of Córdoba, Campus de Rabanales, Edificio Marie Curie, Córdoba, Spain E-14014

^bDepartment of Interfaces, Max Planck Institute of Colloids and Interfaces, Science Park Golm, 14476 Potsdam, Germany

^cGroupe d'Etude des Vecteurs Supramoléculaires du Médicament, Faculté de Pharmacie, Université de Lorraine, CNRS, UMR 7565, 5, Rue Albert Lebrun, BP 80403, 54001 Nancy Cedex, France

S Supporting Information

ABSTRACT: The design of new molecules with directed interactions to functional molecules as complementary building blocks is one of the main goals of supramolecular chemistry. A new *p*-*tert*-butylcalix[6]arene monosubstituted derivative bearing only one alkyl chain with an acid group (C6A3C) has been synthesized. The C6A3C has been successfully used for building Langmuir monolayers at the air–water interface. The C6A3C molecule adopts a flatlike orientation with respect to the air–water interface. The molecular structure gives the molecule amphiphilic character, while allowing the control of both the dissociation degree and the molecular conformation at the air–water interface. The C6A3C has been combined with pristine fullerene (C60) to form the supramolecular complex C6A3C:C60 in 2:1 molar ratio (CFC). The CFC complex retains the ability of C6A3C to form Langmuir monolayers at the air/water interface. The interfacial molecular arrangement of the CFC complex has been convincingly described by in situ UV–vis reflection spectroscopy and synchrotron X-ray reflectivity measurements. Computer simulations complement the experimental data, confirming a perpendicular orientation of the calixarene units of CFC with respect to the air–water interface. This orientation is stabilized by the formation of intermolecular H-bonds. The interfacial monolayer of the CFC supramolecular complex is proposed as a useful model for the well-defined self-assembly of recognition and functional building blocks.



1. INTRODUCTION

Calixarene chemistry has been established as a readily available molecular platform to build a wide variety of interesting cavity-containing and multifunctional molecules. Calixarene derivatives have been widely used as recognition agents. The main interest of calixarenes is based on their broad potential for the design of supramolecular host–guest structures. The supramolecular structures are of high relevance for selective molecular recognition of biologically relevant species, metal cation complexation, design and synthesis of enzyme-mimic systems, or gas sensing.^{1,2}

Supramolecular architectures combining electron-deficient fullerenes and calix[n]arene derivatives are of large interest for applications in the purification of fullerenes.^{3–5} Supramolecular complexes of fullerenes with recognition-active molecules as host–guest entities have been described in both aqueous^{6,7} and organic solvents, where weak charge transfer (CT) forces play an important role in the complexation.^{8–10}

The conformational mobility of calixarenes is a remarkable feature. *p*-*tert*-butylcalix[6]arene might display up to eight conformations: ‘cone’ and ‘partial cone’, which differ in the respective orientation of the aromatic rings. The conformational freedom is a key factor in the optimization of the

particular host–guest interactions between calixarene ligands and their guests.¹¹ Calixarene derivatives have been developed as efficient recognition agents for fullerene.^{12,13} Indeed, the rationale design and synthesis of receptors for fullerene is a current topic of research.^{14,15} The interested readers are referred to the review by Pérez and Martin.¹⁶

The study of calixarenes at the air/water interface provides useful information on their conformation and complexation ability in a very simple and straightforward way. The conformational insights attained at the air/water interface are in agreement with results obtained by using more complex techniques.^{17–20} The use of calixarenes with amphiphilic character offers the advantage of an additional structural factor allowing a certain control in the organization and molecular conformation.

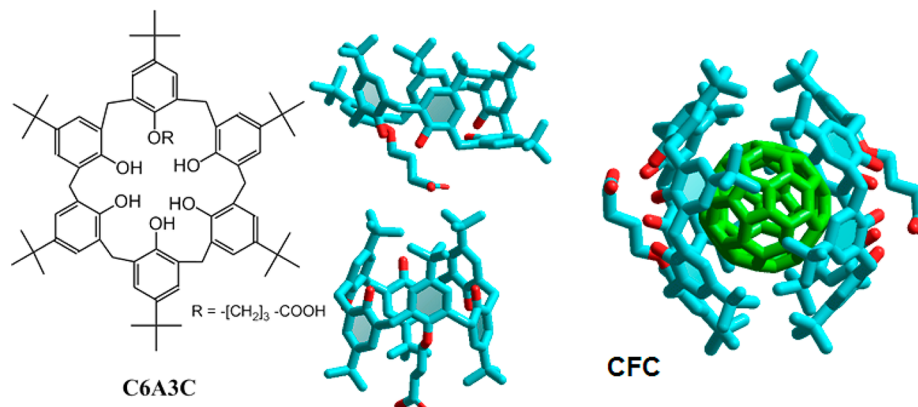
In this work, a monosubstituted asymmetric derivative of *p*-*tert*-butylcalix[6]arene has been synthesized. One of the six –OH groups is replaced by a –O–(CH₂)₃COOH (see Scheme 1, left). The synthesized compound will be named as C6A3C

Received: June 15, 2012

Revised: August 1, 2012

Published: August 2, 2012

Scheme 1. (Left) Molecular Structure of C6A3C; (Center) Two Structures Obtained from MM Geometry Optimization Corresponding to the Cone and OH-Alternate Conformation; (Right) MM Geometry Optimization Structures Obtained for the C6A3C:C₆₀ = 2:1 Complex (CFC)



herein. Symmetrical derivatives of calix[*n*]arenes in which all -OH groups were replaced by $\text{-O-(CH}_2\text{)}_n\text{COOH}$ have been already studied.^{21,22} These symmetric compounds were highly amphiphilic, although the overcrowding of the acid groups prevented adequate control of the degree of dissociation and conformation at the air–water interface.^{23,24} The aim in synthesizing the derivative C6A3C is the fine tuning of both the conformation and the degree of dissociation. Thus, the existence of only one acid group per calix[6]arene unit gives the C6A3C amphiphilic character. Remarkably, given the existence of a single alkyl chain in the C6A3C molecule, the calix[6]arene ring displays great flexibility. This flexibility results in a variety of conformational changes that might be induced by the anisotropy or the applied surface pressure at the air–water interface.

The calyx[6]arene molecule has been selected as a host building block mainly according to the following two points. First, the C₆₀ molecule forms isostructural complexes with calix[6]arene calix:C₆₀ in molar ratio 2:1. In these complexes, the fullerene molecule resides in the inner cavity formed by the double-cone conformation of the calix[6]arene molecules.²⁵ The aggregation of the C₆₀ molecules is prevented. Second, the well-defined inner cavity formed by the calix[6]arene molecules has a size that matches very accurately the C₆₀ molecule. Therefore, the association constant for these types of supramolecular complexes is of a high value. On the other hand, calyx[8]arenes derivatives as *p*-*tert*-butylcalix[8]areneH8 forms a 1:1 complex with C₆₀ in water. However, the C₆₀ molecule was readily expelled from the supramolecular complex by the addition of chloroform.³⁴

The flexibility of the C6A3C molecule might lead to several conformations coexisting at the air–water interface. The variation of the induced surface pressure and the composition of the aqueous subphase, i.e., through ion complexation, might lead to a certain control over the conformational changes.¹⁷ The formation of inclusion complexes can be used to set a specific conformation.¹⁹ In this work we have formed the inclusion complex C6A3C:C₆₀, with a 2:1 stoichiometry. The physicochemical properties of the complex at the air–water interface have been described.

2. EXPERIMENTAL SECTION

2.1. Materials. Pure chloroform as spreading solvent was obtained from Sigma-Aldrich and used as received. Toluene for the CFC

synthesis was purchased from Across Organics (extra dry with molecular sieves, water <50 ppm) and used as received. Ultrapure water, produced by a Millipore Milli-Q unit, pretreated by a Millipore reverse osmosis system (>18.2 MΩcm), was used as subphase.

2.2. Synthesis. ¹H- and ¹³C NMR spectra were recorded on a Bruker DRX 400 (chemical shifts in ppm). Mass spectra (and electrospray ionization - ESI) were recorded on a Bruker micrOTOF-Q apparatus, at the Service Commun de Spectrométrie de Masse Organique, Nancy, or on a Varian Mod 1200 L (Triple quadrupole) at Servicio Central de Apoyo a la Investigación, Córdoba. Infrared was performed on a Mattson Research Series instrument or a Bruker Vector 22 apparatus (KBr, ν in cm^{-1}). Elemental analyses were performed at the Service de Microanalyse, Nancy. Merck TLC plates were used for chromatography analysis (SiO₂, ref 1.05554; Al₂O₃, ref 1.05581). Hexa-*p*-*tert*-butyl-calix[6]arene and other reactants were commercially available and used as received.

2.3. Synthesis of Calixarene Monocarboxyl Derivative.

2.3.1. 5,11,17,23,29,35-Hexakis-*tert*-butyl-calix[6]arene-39,39,40,41,42-pentol-37-[4-(ethylbutyrate)] (1). Hexa-*p*-*tert*-butyl-calix[6]arene (2 g, 2.06 mmol) was dissolved in CH₃CN and refluxed for half an hour in the presence of NaHCO₃ (0.173 g, 2.00 mmol) and K₂CO₃ (0.142 g, 1.03 mmol). Then, 4-bromo-ethylbutyrate (0.294 mL, 2.05 mmol) was added to the mixture, and the reflux was kept for 30 h under Ar. After evaporation of the solvent, the residue was dissolved in CH₂Cl₂ and filtered to remove inorganic salts. The concentrated filtrate was chromatographed (SiO₂; CH₂Cl₂/MeOH 1:1) to give the monoethylester derivative **1** (0.466 g, 20.4%). White solid. IR (pure; ATR): 1732 (C=O). ¹H NMR (CDCl₃): 0.89 (t, *J* = 6.8 Hz, 3 H, OCH₂CH₃); 1.15 (s, 9 H, Me₃C); 1.21 (s, 9 H, Me₃C); 1.26 (s, 18 H, Me₃C); 1.28 (s, 18 H, Me₃C); 2.39 (m, 2 H, OCH₂CH₂CH₂COO⁻); 2.94 (t, *J* = 7.1 Hz, 2 H, OCH₂CH₂CH₂COO⁻); 3.45 (d, *J* = 14.1 Hz, 2 H, Ar-CH₂-Ar); 3.51 (d, *J* = 13.6 Hz, 2 H, Ar-CH₂-Ar); 3.57 (d, *J* = 14.4 Hz, 2 H, Ar-CH₂-Ar); 3.99 (d, *J* = 13.8 Hz, 2 H, Ar-CH₂-Ar); 4.15 (q, *J* = 7.3 Hz, OCH₂CH₃); 4.21–4.29 (m, 4 H, Ar-CH₂-Ar + OCH₂CH₂CH₂COO⁻); 4.30 (d, *J* = 13.6 Hz, 2 H, Ar-CH₂-Ar); 7.06 (s, 2 H, ArH); 7.076 (s, 2 H, ArH); 7.09–7.17 (s + AB, 8 H, ArH). ESI-MS (CH₃CN + HCOOH): 1109.68 ([M + Na]⁺); 2197.38 ([2 M + Na]⁺). Anal. Calcd. For C₇₂H₉₄O₈: 0.3 CH₂Cl₂ (1112.99): C, 78.02; H, 8.57; O, 11.77; found: C 78.32, H 8.10.

2.3.2. 5,11,17,23,29,35-Hexakis-*tert*-butyl-calix[6]arene-39,39,40,41,42-pentol-37-[4-(butyric)] Acid (C6A3C). A mixture of calixarene monoester **1** (0.3 g; 0.269 mmol) and 0.22 mL of 15% NaOH aqueous solution (0.825 mmol) in ethanol (25 mL) was refluxed at 85 °C for 8 h. Then, ethanol was removed under reduced pressure and water was added to the solid residue. HCl (1 M) was added until pH = 1 was raised. The resulting solid was recovered by filtration and dissolved in CH₂Cl₂ (20 mL). This solution was washed with 1 M HCl (20 mL) and brine (20 mL). The organic phase was

recovered, dried over Na_2SO_4 , and evaporated to dryness to give **C6A3C** as a white solid (0.248 g, 85.5%). IR (KBr pellets): 1748, 1716 ($\text{C}=\text{O}$). ^1H NMR ($\text{DMSO}-d_6$): 1.02 (s, 9 H, Me_3C); 1.07 (s, 18 H, Me_3C); 1.13 (s, 9 H, Me_3C); 1.15 (s, 18 H, Me_3C); 2.11 (m, 2 H, $\text{OCH}_2\text{CH}_2\text{CH}_2\text{COO}^-$); 2.57 (t, $J = 7.25$ Hz, 2 H, $\text{OCH}_2\text{CH}_2\text{CH}_2\text{COO}^-$); 3.47–4.23 (m, 14 H, $\text{Ar-CH}_2\text{-Ar} + \text{OCH}_2\text{CH}_2\text{CH}_2\text{COO}^-$); 6.80–7.09 (m, 10 H, ArH); 7.15 (s, 2 H, ArH); 7.99 (s, 2 H, OH); 8.07–8.30 (m, 3 H, OH); 12.06 (br s, COOH). ESI-MS (CH_3CN): 1060 ($[\text{M} + \text{H}]^+$); 1077 ($[\text{M} + \text{NH}_4]^+$). Anal. Calcd. For $\text{C}_{70}\text{H}_{90}\text{O}_8$, 0.25 CH_2Cl_2 (1080.69): C 78.08, H 8.44; found: C 78.29, H 8.03.

2.4. Methods. Langmuir monolayers of **C6A3C** and **CFC** were prepared on pure water at 21 °C. After evaporation of the organic solvent, the monolayer was compressed or expanded using a movable barrier on a Nima rectangular trough provided with a filter paper Wilhelmy plate with a compression velocity of $10\text{--}20 \text{ \AA}^2 \text{ molecule}^{-1} \text{ min}^{-1}$, allowing the recording of surface pressure–area (π – A) isotherms. The system was also equipped with a vibrating capacitor device, Kelvin Probe SP1 (Nanofilm Technologies, Göttingen, Germany) for measurement of the surface potential/area (ΔV – A).

Brewster angle microscopy (BAM) was used to gain additional information on the molecular organization of **C6A3C** and **CFC** in monolayers at the air–water interface. Images of the film have been recorded with a lateral resolution of $2 \mu\text{m}$ (I-Elli2000 supplied by NFT, Accurion GmbH, Göttingen, Germany). The image processing procedure included a geometrical correction of the image, as well as a filtering operation to reduce interference fringes and noise. Furthermore, the brightness of each image was scaled to improve contrast. The size of the images is $430 \mu\text{m}$ in width. The microscope and the film balance were located on a table with vibration isolation (antivibration system MOD-2 S, Accurion GmbH, Göttingen, Germany) in a large class 100 clean room.

UV–visible reflection spectra at normal incidence as the difference in reflectivity (ΔR) of the film-covered water surface and the bare surface were obtained with a *ref SPEC*² surface analysis spectrometer, supplied by Accurion GmbH, Göttingen, Germany.

Specular X-ray reflectivity (XRR): The specular X-ray reflectivity (XRR) measurements were performed on the undulator beamline BW1 at HASYLAB, DESY (Hamburg, Germany). XRR provides an averaged electron density profile normal to the interface of all molecules. For reflectivity measurements, the angles of incidence α_i and reflected α_f beams are equal and varied in a range $0.5\alpha_c < \alpha_i$ (α_f) $< 30\alpha_c$, where $\alpha_c = 0.138$. The reflected intensity was measured by a NaI scintillation detector in the plane of incidence as a function of the vertical scattering vector component Q_z . The electron density profile was obtained from the reflectivity curve using a linear combination of b-splines following the approach of Pedersen and Hamley. The electron density profiles were calculated using the StochFit software.²⁶

2.5. Molecular Mechanics Study. The molecular mechanics simulations were carried out using the HyperChem molecular modeling package.²⁷ The geometry of the molecule was preoptimized using the Amber96 force field with no partial charges. Then the charges were assigned using the AM1 semiempirical method. Next, the geometry was again optimized using Amber. The procedure was repeated until the convergence was achieved (the convergence criteria for geometrical optimization was $0.001 \text{ kcal}/(\text{\AA}\cdot\text{mol})$). A similar method of assigning partial charges was used for other calixarene derivatives.^{22,28,29} After charges were assigned, three runs of the molecular dynamics simulations were performed to search for the possible existence of other structures with lower energy. Each run consisted of heating the structure to 300 K, molecular dynamics simulations for 5 ps, and then annealing to 0 K.

C6A3C molecule has 20 different conformations, depending on the relative orientation of the $-\text{OH}$ groups respect to the acid group. The molecular geometry optimization in vacuum was performed starting from some of these conformations. Scheme 1 (center) shows two of the structures obtained starting from the conformation cone and OH -alternate, respectively. The energies of the found structures were very similar in all runs. Often the formation of hydrogen bonds contributes to the stability of the species. Moreover, our results show that the

formation of the inclusion complex between **C6A3C** and **C₆₀** is possible only when the calix[6]arene is in cone conformation. The structure obtained with **C6A3C**:**C₆₀** = 2:1 stoichiometry is stable and corresponds to a true energy minimum. The structure obtained for the 2:1 complex is shown in Scheme 1 (right). In this representation, hydrogen atoms are not drawn and the **C₆₀** is green colored in order to distinguish the different molecules.

3. RESULTS AND DISCUSSION

3.1. Synthesis of Calixarene–Fullerene Complex CFC.

A mixture 2 mM of **C6A3C** and 1 mM **C₆₀** in toluene was refluxed at 140 °C for 24 h. A change of the color of the solution from violet to brown was observed. This change of color is indicative of the formation of the supramolecular complex. The obtained product was used without further purification. In Figure 1, UV–vis spectra of **C₆₀** (1 mM, red

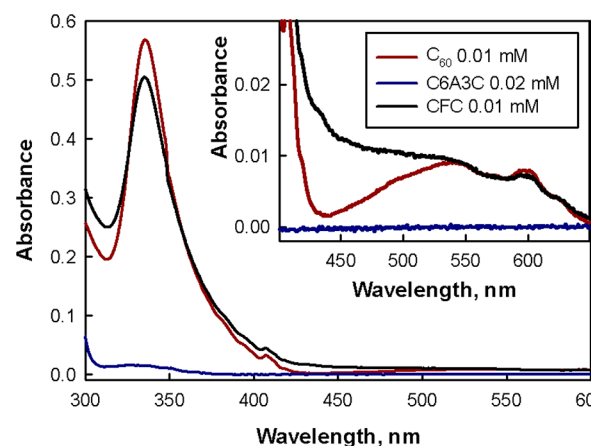


Figure 1. UV–vis spectrum (toluene solutions) of **C₆₀** 0.01 mM (red line); **C6A3C** 0.02 mM (blue line); and **CFC** 0.01 mM [**C6A3C** 0.02 mM + **C₆₀** 0.01 mM] (black line).

line) and **C6A3C** (2 mM, blue line) in toluene solution are shown. Also, Figure 1 shows the UV–vis spectra of the **C6A3C**:**C₆₀** = 2:1 complex (black line), named as **CFC** herein. The **CFC** concentration was 1 mM (2 mM in **C6A3C** and 1 mM in **C₆₀**). There is a large spectroscopic change in the region from 420 to 480 nm due to the charge transfer (CT) absorption band between the **C₆₀** and the calixarenes, indicating the formation of the complex.^{30,31} In order to confirm the stoichiometry of the complex, the increase of the absorption at 437 nm vs mole fraction of **C₆₀** (for a constant concentration of **C₆₀**) was analyzed, obtaining the maxima variation for the 2:1 stoichiometry,³¹ see Figure S1 in the Supporting Information.

According to previous reports by other researchers and our UV–vis data in solution for different molar ratios, we concluded that the **C6A3C**:**C₆₀** 2:1 molar ratio is optimal for the complexation of the **C₆₀** and **C6A3C** molecules. Therefore, the usage of alternative molar ratios for fabricating a Langmuir monolayer would lead to a certain fraction of **C6A3C**:**C₆₀** 2:1 supramolecular complex units and the excess of either **C6A3C**:**C₆₀** at the air–water interface. In such a case, phase separation and a mixture of aggregates is expected. This work is aimed at the design and characterization of a Langmuir monolayer of a pure and well-defined supramolecular complex. Therefore, we use exclusively **C6A3C**:**C₆₀** supramolecular complex in 2:1 molar ratio.

3.2. Surface Pressure/Area Isotherms. Figure 2 shows the surface pressure–molecular area (π – A) isotherms of the

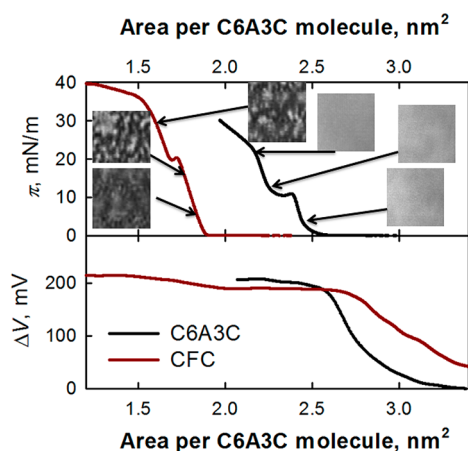


Figure 2. (Top) Surface pressure–molecular area (π – A) isotherms of C6A3C (black line) and CFC (red line). BAM images are shown under different surface pressures. Image size: $42\ \mu\text{m}$ width. (Bottom) Surface potential–area (ΔV – A) isotherms of C6A3C (black line) and CFC (red line).

C6A3C molecule and the CFC supramolecular complex. The molecular area is expressed as surface area per C6A3C molecule in both cases. The Langmuir monolayer formed by pure C6A3C shows the overshoot of the surface pressure at a molecular area of $\sim 2.6\ \text{nm}^2/\text{molecule}$. This value is indicative of a parallel orientation of C6A3C with respect to the air–water interface.¹⁷ Scheme 2 shows an idealized representation of the C6A3C cone conformation and its interfacial projected area. The interaction between the hydrophilic region of the C6A3C (i.e., the OH and acidic groups) and water favors the cone conformation. However, different conformations might coexist at the air–water interface. The presence of the terminal acid group in the alkyl chain is sufficient to induce a parallel orientation of the C6A3C plane to the air–water interface for any given conformation of the calixarene molecule. The pure *tert*-butyl-calix[6]arene monolayer in the absence of complex-forming ions in the subphase leads to a perpendicular conformation of the main plane of the molecule at the air–water interface.^{17,32}

For a surface pressure of $10\ \text{mN/m}$ the C6A3C isotherm shows a change of slope, being characteristic of other *p*-*tert*-butylcalix(6)arene derivatives. This change of slope has been attributed to a conformational phase transition. Upon further compression of the Langmuir monolayer, a continuous rise of the isotherm resembling those presented by condensed phase is detected. There is no clear starting point of the one-phase

region. For surface pressures above $22\ \text{mN/m}$, there is a decrease in slope of the π – A isotherm. This decrease in the slope cannot be related to a typical amphiphilic monolayers collapse, i.e., strong reduction of the surface area. This behavior has been related to a gradual loss of parallel orientation toward a more compact perpendicular orientation at $\sim 1.8\ \text{nm}^2$ per molecule, see Scheme 2.¹⁷

The complexation of the C_{60} molecule by two calixarene molecules leads to the supramolecular complex named as CFC, see Scheme 2. The surface pressure–molecular area isotherm of CFC is clearly different from that of pure C63AC. For CFC the surface pressure starts to rise at an area of $\sim 1.9\ \text{nm}^2$ per C6A3C molecule. This value is indicative of a perpendicular orientation of C6A3C with respect to the air–water interface (see Scheme 2). It also indicates that the C_{60} occupies no net area at the interface, which supports the idea of the formation of the inclusion complex.

The change of slope in the isotherm is observed at a surface pressure of $\sim 20\ \text{mN/m}$. A typical collapse is observed at a surface pressure of $\sim 36\ \text{mN/m}$. The perpendicular orientation of C6A3C units is stabilized by means of the formation of intermolecular H-bonds.

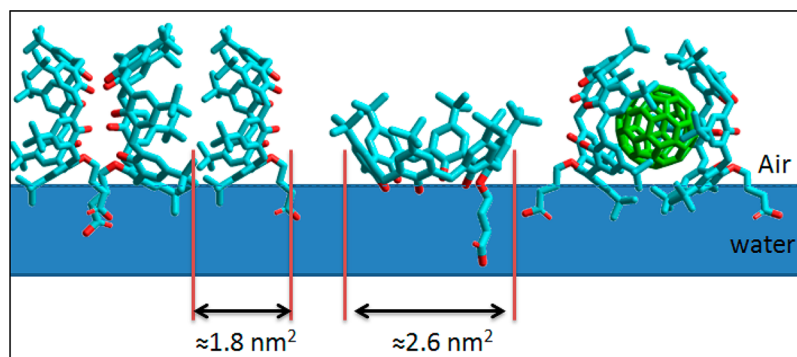
Cyclic isotherms of the CFC supramolecular complex have been performed. A small hysteresis between the first and second isotherm compression cycles is observed. The reduction of area per molecule at a constant value of surface pressure is $\sim 0.04\ \text{nm}^2$, see Figure S2 in the Supporting Information. This hysteresis decreases in the case of not reaching the collapse surface pressure during the first compression process.

3.3. Brewster Angle Microscopy. The morphology of both monolayers was directly visualized by Brewster angle microscopy (BAM) simultaneously with the π – A isotherm recording. The Langmuir monolayer of pure C6A3C is completely homogeneous along the whole isotherm. However, the Langmuir monolayer of pure CFC shows a completely different morphology, with irregular bright and dark regions in an uneven fashion.

The absence of domains or micrometer structure in the monolayer of C6A3C might be due to the parallel orientation adopted by the ring of calix[6]arene. Indeed, in this orientation the interactions between molecules are weak, and hydrogen bonds can be formed only intramolecularly and with water molecules in the subphase. This situation does not favor the formation of large domains that could be visualized by BAM.

On the contrary, in the case of the monolayer of the complex CFC the interactions between neighboring molecules are strong due to the perpendicular orientation of the calix[6]arene

Scheme 2. Idealized Representation of the Interface Projected Area for the Cone Conformation of C6A3C, and CFC



ring, enabling the formation of intermolecular hydrogen bonding. The UV–vis reflection spectra point to the absence of aggregation of the fullerene molecules in the CFC Langmuir monolayer. Therefore, the domains observed by BAM should correspond to micrometric aggregates of CFC supramolecular complexes. The densest aggregates are seen in the BAM pictures as the bright regions. On the other hand, less dense aggregates are observed as dark domains. No occurrence of dissociation of the complex and fullerene separation is expected, as shown by the UV–vis reflection spectra. Therefore, the observed structures are due to the lateral aggregation between the C6A3C units.

3.4. Surface Potential–Area Isotherms. The surface potential of a Langmuir monolayer depends on three main factors: (a) the vertical component of the dipole moments of the monolayer molecules, (b) the relative orientation of the water molecules, and (c) the ionic environment and the state of the headgroups and subphase. The first of these factors is very sensitive to molecular reorientations at the air–water interface. Therefore, the surface potential measurements of the C63AC and CFC monolayers are of high interest. Note that the information provided is only qualitative. Figure 2 shows the ΔV vs A per C6A3C molecule for the C6A3C and CFC monolayers.

The π – A isotherm and the surface potential display opposite trends with the compression of the monolayers. The surface pressure begins to increase for larger values of molecular areas for the case of the C6A3C when compared to the CFC monolayer. On the contrary, the surface potential rises and reaches a first plateau for larger area values in the case of the CFC monolayer. Thus, for the monolayer of pure C6A3C the surface potential starts to rise at an area of $\sim 3.30 \text{ nm}^2$ per C6A3C molecule and reaches a plateau at a surface potential of $\sim +210 \text{ mV}$ at 2.60 nm^2 per C6A3C molecule. This value of molecular area is coincident with the overshoot of surface pressure. This behavior suggests that the calixarene molecule does not adopt a single conformation when spread on the air–water interface. Only the application of surface pressure induces the parallel conformation of the molecule. However, in the case of CFC monolayer the ΔV is different from zero even at a large value of molecular area of $\sim 3.5 \text{ nm}^2$ per C6A3C molecule, reaching a first plateau of $\sim +180 \text{ mV}$ at areas of 2.8 nm^2 per C6A3C molecule. Upon further compression of the monolayer, the surface potential is approximately constant until an area of $\sim 1.9 \text{ nm}^2$ per C63AC molecule is reached, coincident with the overshoot of surface pressure. In the final stage of the isotherm the ΔV increased slightly up to values of surface potential of $\sim +210 \text{ mV}$. This behavior suggests that the CFC complex adopts a defined conformation before the surface pressure begins to increase significantly.

The maximum values of ΔV are coincident for both monolayers, $\sim +210 \text{ mV}$ at the maximum stage of compression of the monolayer. Although this coincidence in the value of surface potential seems to be in contradiction with the different orientations models for the C6A3C and CFC monolayers, it can be attributed to the effect of the headgroup. In the case of no buffer in the subphase, i.e., neutral pH, the carboxylic group of the C63AC molecule should be partially dissociated. The orientation of the carboxylic group is assumed to be the main contribution to the total effective dipole moment of the whole monolayer at the air–water interface. In this scenario, the change in the orientation of the hydrophobic region of the C63AC molecule does not contribute significantly to the total

value of surface potential. Therefore, the coincidence in the value of surface potential indicates the same orientation of the carboxylic group for both C63AC and CFC monolayers.

3.5. In Situ UV–Vis Reflection Spectroscopy at the Air–water Interface. In order to obtain direct evidence of the presence of the C_{60} molecule in the CFC Langmuir monolayer, UV–vis reflection spectra were acquired. Figure 3 shows the UV–vis reflection spectra recorded at $\pi = 5, 15$, and 30 mN/m . The UV–vis spectrum of CFC in toluene solution is included in Figure 3 for comparison.

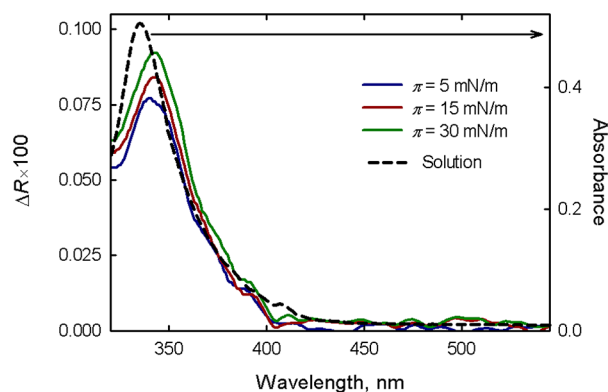


Figure 3. UV–vis reflection spectra (ΔR) of the CFC monolayer obtained at different surface pressures (solid lines). (Blue) 5 mN/m , (red) 15 mN/m , (green) 30 mN/m . For comparison, the absorption spectrum of CFC 0.01 mM on toluene solution (dashed line) is also shown.

The UV–vis reflection spectra show a small red-shift from the 335 nm band in solution to the 341 nm at the air–water interface. This shift may be related to the aggregation of C_{60} and/or to the different environments existing in the monolayer and in the toluene solution. In most of the cases, C_{60} aggregation can be detected by the presence of a broad band centered around 450 nm .^{33,34} However, this band has been not observed in the experiments presented herein. Remarkably, the width of the band at 341 nm at the air–water interface is very similar to that obtained in solution. Due to the limited resolution of the UV–vis reflection spectra, the charge transfer bands could not be detected, see Figure 1. Note that the UV–vis reflection spectra recorded at the air/water interface correspond to a single monolayer. Additionally, the bands present at 550 and 600 nm corresponding to the fullerene molecules could not be observed. Note that the absorption molar coefficient of the mentioned bands is ~ 50 lower than the main band of the fullerene molecule at $\sim 340 \text{ nm}$, see Figure 1. The band corresponding to the charge transfer is detected in bulk solution by the increase of absorbance at a wavelength of 437 nm of the CFC complex when compared to the fullerene molecule. However, we lack the UV–vis reflection spectrum of the fullerene molecule as a reference, given that the pure fullerene molecule does not form Langmuir monolayers. Therefore, the comparison performed for the spectra in bulk solution could not be performed using the UV–vis reflection spectra. Remarkably, the UV–vis reflection data allow the in situ stability test of the CFC complex. In case of a breakage of the supramolecular complex, the aggregation of fullerene units at the air–water interface is most likely to take place. By ruling out the aggregation of fullerene molecules at the air–water

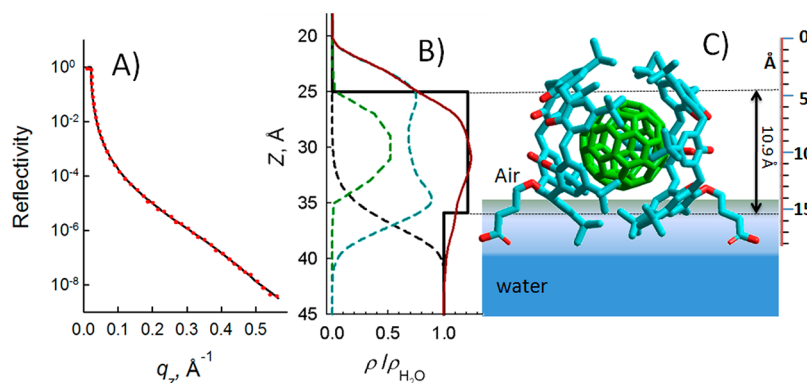


Figure 4. (Left) X-ray reflectivity for CFC monolayer at 30 mN/m (red dot) and numerical fit using one box model (black solid line). (Center) Vertical profile of the relative electron density obtained from the numerical fit (black solid line) and from the spatial molecular distribution (red solid line). The profiles of the relative electron density for C60 (dashed green line) and C6A3C (dashed cyan line) are also shown. The dashed black line represents the electron density of water. (Right) The vertical spatial distribution of CFC used to determine the relative electron density.

interface, the possibility of a nonstable CFC supramolecular complex is ruled out.

For low values of absorption, the reflection ΔR is given in a reasonable approximation by^{35,36}

$$\Delta R = 2.303 \times 10^3 \cdot \Gamma_{\text{C60}} \cdot f_{\text{orient}} \cdot \epsilon \cdot \sqrt{R_s} \quad (1)$$

where Γ_{C60} is the surface concentration of C_{60} in mol cm^{-2} , $R_s = 0.02$ is the reflectivity of the air–water interface at normal incidence,³⁷ ϵ is the extinction coefficient given as $\text{L mol}^{-1} \text{cm}^{-1}$, and f_{orient} is a numerical factor that takes into account the different average orientations of the chromophores in solution as compared to the monolayer at the air–water interface, which could be considered $f_{\text{orient}} = 1$ for pseudospherical molecules.^{38,39}

The maximum value of reflection at $\pi = 30 \text{ mN/m}$ (341 nm, see Figure 3) is $\Delta R \approx 9.2 \times 10^{-4}$. From the CFC spectrum in toluene solution, we can obtain $\epsilon \approx 5.0 \times 10^4 \text{ L mol}^{-1} \text{cm}^{-1}$ at 335 nm. This value is used herein, assuming no aggregation. Therefore, $\Gamma_{\text{C60}} \approx 5.6 \times 10^{-11} \text{ mol cm}^{-2}$ is obtained from eq 1.

The surface area of the CFC monolayer is 1.55 nm^2 per C6A3C molecule at $\pi = 30 \text{ mN/m}$, from the surface pressure–molecular area isotherm. Therefore, the surface concentration of calix[6]arene is $\Gamma_{\text{C6A3C}} = 10^{14}/A_{\text{NA}} \approx 1.1 \times 10^{-10} \text{ mol cm}^{-2}$, where N_A is the Avogadro number. Given the 2:1 stoichiometry of the C6A3C: C_{60} supramolecular complex, the surface concentration of the C_{60} molecule is calculated as $\Gamma_{\text{C60}} \sim 5.05 \times 10^{-11} \text{ mol cm}^{-2}$. This value of surface area is in good agreement with the value previously obtained from the UV–vis reflection spectrum.

The aggregation of pristine C_{60} molecules leads to a decrease in molar extinction coefficient at 335 nm, as reported in previous studies.^{33,34} This decrease in the absorption properties of the CFC complex does not take place in the experiments presented herein, thereby confirming that there is no aggregation of the fullerene molecules.

3.6. Synchrotron-Based in Situ X-ray Reflectivity (XRR). XRR experiments allow the determination of the vertical electron density profile of soft matter thin films.^{40,41} The data for $\pi = 30 \text{ mN/m}$ show a single decreasing reflectivity (Figure 4, left). The experimental data have been modeled using a one box model using StochFit software.²⁶ The numerical fit of the experimental data allows obtaining a thickness of $10.9 \pm 0.5 \text{ \AA}$, and a relative electron density with

respect to bulk water of $\rho/\rho_{\text{water}} = 1.21 \pm 0.02$, considering an interfacial roughness of $3.42 \pm 0.07 \text{ \AA}$, see Figure 4, center.

The vertical profile of electron density was determined from the spatial distribution of different atoms that HyperChem provided after geometry optimization of the complex.²⁷ Thus, in Figure 4 center, the green dashed line represents the relative electron density of C60, and the cyan dashed line represents the relative electron density of the two C6A3C units. The dashed black line represents the electron density of water which is fitted to a Gaussian distribution for the contact region with the CFC monolayer. Finally, the overall relative electron density is represented as a red solid line.

The vertical thickness of the CFC complex is $\sim 18 \text{ \AA}$, see Figure 4. The CFC complex can be considered as three different regions; the central region of $\sim 8 \text{ \AA}$ shows a high electron density, which reaches a maximum of approximately 1.25 times the electron density of water. The two external regions of $\sim 5 \text{ \AA}$ display a steep decrease of the electron density with the distance from the central region of the CFC complex.

The region which is in contact with water should be partially hydrated; therefore, the electron density should tend quickly to unity. The one box model represents a good approximation to the electron density profile obtained theoretically, which is a further evidence of the formation of the inclusion complex. Exclusively the formation of the CFC complex is able to explain the existence of a 11 \AA thickness region with an electron density 1.2 times higher than the electron density of water.

4. CONCLUSIONS

In this work, a novel monosubstituted asymmetric derivative of *p*-*tert*-butylcalix[6]arene has been synthesized: C63AC. One of the six -OH groups is replaced by a -O-(CH₂)₃COOH group. The existence of only one acid group per molecule in the C6A3C derivative gives amphiphilic character to the C63AC molecule. Moreover, the dissociation degree of the carboxylic group can be tuned to a certain extent.

The C6A3C molecule has been studied, both alone and in combination with fullerene (C_{60}) at the air–water interface. The supramolecular complex C6A3C: C_{60} 2:1 (CFC) has been synthesized prior to spreading on the air–water interface. The formation of this inclusion complex and the stoichiometry has been studied by UV–vis spectroscopy, confirming the C6A3C: $\text{C}_{60} = 2:1$. Charge transfer between the C_{60} and the calixarenes has been found. The molecular conformation of

both C63AC and CFC monolayers has been described by a combination of experimental and computational methods.

The C6A3C molecule adopts a parallel orientation of the main plane with respect to the air–water interface. In the case of the CFC complex, the C6A3C units adopt perpendicular orientation with respect to the air–water interface. The absence of expansion in the surface pressure–molecular area isotherm confirms the formation of the inclusion complex between the C₆₀ and the C63AC molecules. The perpendicular orientation of C6A3C units is stabilized by intermolecular H-bonds. Direct evidence of the presence of C₆₀ in the CFC monolayer is obtained by in situ UV–vis reflection spectra. The UV–vis reflection spectra discard aggregation of the C₆₀ molecules. The vertical electron density profile of CFC monolayer was determined using in situ synchrotron-based X-ray reflectivity measurements. A good agreement of the experimental data with the theoretical electron density profile for the inclusion complex was found.

We expect the inclusion complex calixarene:fullerene at the air–water interface to be useful as a model for the well-defined supramolecular structures containing both recognition and photofunctional molecules.

■ ASSOCIATED CONTENT

■ Supporting Information

Relative difference of absorption at a wavelength of 437 nm of a mixed solution containing C63AC and C60 molecules with respect to pure fullerene molecule vs the mole fraction of C₆₀ in the mixed solution. Cyclic isotherms of the CFC supramolecular complex. This material is available free of charge via the Internet at <http://pubs.acs.org>.

■ AUTHOR INFORMATION

Corresponding Author

*Fax/Tel: +34 957 218 618. E-mail: lcamacho@uco.es.

Notes

The authors declare no competing financial interest.

■ ACKNOWLEDGMENTS

We thank the Spanish CICYT for financial support of this research in the framework of Project CTQ2010-17481 and also thank the Junta de Andalucía (Consejería de Innovación, Ciencia y Empresa) for special financial support P08-FQM-4011 and P10-FQM-6703. A.G-D., thanks the Ministerio de Ciencia e Innovación for a predoctoral grants (FPI program). J.J.G.-C. acknowledges Alexander von Humboldt Foundation for a postdoctoral fellowship. HASYLAB at DESY and Dr. Bernd Struth are acknowledged for excellent beamtime and support.

■ REFERENCES

- (1) Gutsche, C. D. *Calixarenes*; The Royal Society of Chemistry: Cambridge, 1989.
- (2) Asfari, M.-Z.; Böhmer, V.; Harrowfield, J.; Vicens, J. *Calixarenes* 2001; Kluwer Academic: Dordrecht, 2001.
- (3) Suzuki, T.; Nakashima, K.; Shinkai, S. Very Convenient and Efficient Purification Method for Fullerene (C₆₀) with 5,11,17,23,29,35,41,47-Octa-*tert*-butylcalix[8]arene-49,50,51,52,53,54,55,56-octol. *Chem. Lett.* **1994**, 699–702.
- (4) Atwood, J. L.; Koutsantonis, G. A.; Raston, C. L. Purification of C₆₀ and C₇₀ by Selective Complexation with Calixarenes. *Nature* **1994**, 368, 229–231.

- (5) Komatsu, N. Preferential Precipitation of C₇₀ over C₆₀ with *p*-Halohomooxalix[3]arenes. *Org. Biomol. Chem.* **2003**, 1, 204–209.
- (6) Yoshida, Z.; Takekuma, H.; Takekuma, S.; Matsubara, Y. Molecular Recognition of C₆₀ with γ -Cyclodextrin. *Angew. Chem., Int. Ed.* **1994**, 33, 1597–1599.
- (7) Andersson, T.; Nilsson, K.; Sundahl, M.; Westman, G.; Wennerström, O. C₆₀ Embedded in γ -Cyclodextrin: A Water-Soluble Fullerene. *J. Chem. Soc., Chem. Commun.* **1992**, 604.
- (8) Guldi, D. M.; Luo, C.; Prato, M.; Troisi, A.; Zerbetto, F.; Scheloske, M.; Dietel, E.; Bauer, W.; Hirsch, A. Parallel (Face-to-Face) Versus Perpendicular (Edge-to-Face) Alignment of Electron Donors and Acceptors in Fullerene Porphyrin Dyads: The Importance of Orientation in Electron Transfer. *J. Am. Chem. Soc.* **2001**, 123, 9166–9167.
- (9) Haino, T.; Yanase, M.; Fukazawa, Y. New Supramolecular Complex of C₆₀ Based on Calix[5]arene—Its Structure in the Crystal and in Solution. *Angew. Chem., Int. Ed.* **1997**, 36, 259–260.
- (10) Wang, Y.-B.; Lin, Z. Supramolecular Interactions between Fullerenes and Porphyrins. *J. Am. Chem. Soc.* **2003**, 125, 6072–6073.
- (11) Lonetti, B.; Lo Nostro, P.; Ninham, B. W.; Baglioni, P. Anion Effects on Calixarene Monolayers: A Hofmeister Series Study. *Langmuir* **2005**, 21, 2242–2249.
- (12) Guan, A.-J.; Zhang, E.-X.; Xiang, J.-F.; Yang, Q.-F.; Li, Q.; Sun, H.-X.; Wang, D.-X.; Zheng, Q.-Y.; Xu, G.-Z.; Tang, Y.-L. Regulating the Conformation of Methylazacalix[6]pyridine by Oligonucleotide BCL-2 2345 and Its Recognition of Hydroxymethylpiperazinofullerene. *J. Phys. Chem. Lett.* **2012**, 3, 131–135.
- (13) Haino, T.; Hirai, E.; Fujiwara, Y.; Kashiwara, K. Supramolecular Cross-Linking of [60]Fullerene-Tagged Polyphenylacetylene by the Host–Guest Interaction of Calix[5]arene and [60]Fullerene. *Angew. Chem., Int. Ed.* **2010**, 49, 7899–7903.
- (14) Canevet, D.; Pérez, E. M.; Martín, N. Wraparound Hosts for Fullerenes: Tailored Macrocycles and Cages. *Angew. Chem., Int. Ed.* **2011**, 50, 9248–9259.
- (15) Canevet, D.; Gallego, M.; Isla, H.; de Juan, A.; Pérez, E. M.; Martín, N. Macrocyclic Hosts for Fullerenes: Extreme Changes in Binding Abilities with Small Structural Variations. *J. Am. Chem. Soc.* **2011**, 133, 3184–3190.
- (16) Pérez, E. M.; Martín, N. Curves Ahead: Molecular Receptors for Fullerenes Based on Concave–convex Complementarity. *Chem. Soc. Rev.* **2008**, 37, 1512–1519.
- (17) Dei, L.; Casnati, A.; Lo Nostro, P.; Baglioni, P. Selective Complexation by *p*-*tert*-Butylcalix[6]arene in Monolayers at the Water–Air Interface. *Langmuir* **1995**, 11, 1268–1272.
- (18) Dei, L.; Casnati, A.; LoNostro, P.; Pochini, A.; Ungaro, R.; Baglioni, P. Complexation Properties of *p*-*tert*-Butylcalix[6]arene Hexamide in Monolayers at the Water–Air Interface. *Langmuir* **1996**, 12, 1589–1593.
- (19) Dei, L.; LoNostro, P.; Capuzzi, G.; Baglioni, P. Langmuir Films of *p*-*tert*-Butylcalix[8]arene. Conformations at the Water–Air Interface and Complexation of Fullerene C₆₀. *Langmuir* **1998**, 14, 4143–4147.
- (20) Capuzzi, G.; Fratini, E.; Dei, L.; LoNostro, P.; Casnati, A.; Gilles, R.; Baglioni, P. Counterion Complexation of Calixarene Ligands in Monolayers and Micellar Solutions. *Colloids Surf., A* **2000**, 167, 105–113.
- (21) Richardson, T.; Greenwood, M. G.; Davis, F.; Stirling, C. J. M. Pyroelectric Molecular Baskets: Temperature-Dependent Polarization from Substituted Calix(8)arene Langmuir–Blodgett Films. *Langmuir* **1995**, 11, 4623–4625.
- (22) de Miguel, G.; Pedrosa, J. M.; Martín-Romero, M. T.; Muñoz, E.; Richardson, T. H.; Camacho, L. Conformational Changes of a Calix[8]arene Derivative at the Air–Water Interface. *J. Phys. Chem. B* **2005**, 109, 3998–4006.
- (23) de Miguel, G.; Perez-Morales, M.; Martín-Romero, M. T.; Muñoz, E.; Richardson, T. H.; Camacho, L. J-Aggregation of a Water-Soluble Tetracationic Porphyrin in Mixed LB Films with a Calix[8]arene Carboxylic Acid Derivative. *Langmuir* **2007**, 23, 3794–3801.

- (24) de Miguel, G.; Martín-Romero, M. T.; Pedrosa, J. M.; Muñoz, E.; Pérez-Morales, M.; Richardson, T. H.; Camacho, L. Disaggregation of an Insoluble Porphyrin in a Calixarene Matrix: Characterization of Aggregate Modes by Extended Dipole Model. *Phys. Chem. Chem. Phys.* **2008**, *10*, 1569–1576.
- (25) Redshaw, C. Coordination Chemistry of the Larger Calixarenes. *Coord. Chem. Rev.* **2003**, *244*, 45–70.
- (26) Danauskas, S. M.; Li, D.; Meron, M.; Lin, B.; Lee, K. Y. C. Stochastic Fitting of Specular X-ray Reflectivity Data Using StochFit. *J. Appl. Crystallogr.* **2008**, *41*, 1187–1193.
- (27) *Hypercube Hyperchem*, 7.51; Hypercube: Gainesville, FL, U.S.A., 1999.
- (28) Kane, P.; Fayne, D.; Diamond, D.; Bell, S. E. J.; McKervey, M. A. Modelling of the Sodium Complex of a Calixarene Tetraester in the 1,3-Alternate Conformation. *J. Mol. Model.* **1998**, *4*, 259–267.
- (29) Van der Heyden, A.; Regnouf-de-Vains, J. B.; Warszynski, P.; Dalbavie, J. O.; Zywockinski, A.; Rogalska, E. Probing Inter- and Intramolecular Interactions of Six New *p*-*tert*-Butylcalix[4]arene-Based Bipyridyl Podands with Langmuir Monolayers. *Langmuir* **2002**, *18*, 8854–8861.
- (30) Leach, S.; Vervloet, M.; Despres, A.; Breheret, E.; Hare, J. P.; Dennis, T. J.; Kroto, H. W.; Taylor, R.; Walton, D. R. M. Electronic Spectra and Transitions of the Fullerene C60. *Chem. Phys.* **1992**, *160*, 451–466.
- (31) Ikeda, A.; Yoshimura, M.; Shinkai, S. Solution Complexes Formed from C60 and Calixarenes. On the Importance of the Preorganized Structure for Cooperative Interactions. *Tetrahedron Lett.* **1997**, *38*, 2107–2110.
- (32) Ishikawa, Y.; Kunitake, T.; Matsuda, T.; Otsuka, T.; Shinkai, S. Formation of Calixarene Monolayers Which Selectively Respond to Metal Ions. *J. Chem. Soc., Chem. Commun.* **1989**, 736.
- (33) Hungerbühler, H.; Guldi, D. M.; Asmus, D. Incorporation of C60 into Artificial Lipid Membranes. *J. Am. Chem. Soc.* **1993**, *115*, 3386–3387.
- (34) Torres, V. M.; Posa, M.; Srdjenovic, B.; Simplicio, A. L. Solubilization of Fullerene C60 in Micellar Solutions of Different Solubilizers. *Colloids Surf., B* **2011**, *82*, 46–53.
- (35) Grüniger, H.; Möbius, D.; Meyer, H. Enhanced Light Reflection by Dye Monolayers at the Air–water Interface. *J. Chem. Phys.* **1983**, *79*, 3701–3711.
- (36) Pedrosa, J. M.; Martín-Romero, M. T.; Camacho, L.; Möbius, D. Organization of an Amphiphilic Azobenzene Derivative in Monolayers at the Air–Water Interface. *J. Phys. Chem. B* **2002**, *106*, 2583–2591.
- (37) Grüniger, H.; Möbius, D.; Lehmann, U.; Meyer, H. Reflection and Transmission of Light by Dye Monolayers. *J. Chem. Phys.* **1986**, *85*, 4966–4980.
- (38) Huesmann, H.; Bignozzi, C. A.; Indelli, M. T.; Pavanin, L.; Rampi, M. A.; Möbius, D. Organization of a Metal Complex Dyad in Monolayers. *Thin Solid Films* **1996**, *284–285*, 62–65.
- (39) Giner-Casares, J. J.; Pérez-Morales, M.; Bolink, H. J.; Lardiés, N.; Muñoz, E.; de Miguel, G.; Martín-Romero, M. T.; Camacho, L. Segregation of Lipid in Ir-Dye/DMPA Mixed Monolayers As Strategy to Fabricate 2D Supramolecular Nanostructures at the Air–water Interface. *J. Mater. Chem.* **2008**, *18*, 1681–1688.
- (40) Ege, C.; Majewski, J.; Wu, G.; Kjaer, K.; Lee, K. Y. C. Templating Effect of Lipid Membranes on Alzheimer's Amyloid Beta Peptide. *ChemPhysChem* **2005**, *6*, 226–229.
- (41) Evers, F.; Shokuie, K.; Paulus, M.; Sternemann, C.; Czeslik, C.; Tolan, M. Exploring the Interfacial Structure of Protein Adsorbates and the Kinetics of Protein Adsorption: An in Situ High-Energy X-ray Reflectivity Study. *Langmuir* **2008**, *24*, 10216–10221.